Carbohydrate Polymers 83 (2011) 1869–1878

Contents lists available at ScienceDirect

Carbohydrate Polymers

journal homepage: www.elsevier.com/locate/carbpol

Formation of inclusion complexes of starch with fatty acid esters of bioactive compounds

Ursula V. Lay Ma, John D. Floros, Gregory R. Ziegler*

Department of Food Science, The Pennsylvania State University, 202 Food Science Building, University Park, PA 16802, United States

ARTICLE INFO

Article history:
Received 6 August 2010
Received in revised form 19 October 2010
Accepted 22 October 2010
Available online 30 October 2010

Keywords:
Starch
Amylose
Fatty acid esters
Inclusion complex
FTIR
DSC
XRD

ABSTRACT

The formation of amylose, amylopectin, and high amylose maize starch inclusion complexes with ascorbyl palmitate, retinyl palmitate, and phytosterol esters was evaluated. Amylose and high amylose maize starch formed inclusion complexes with the studied fatty acid esters. However, only retinyl palmitate formed a complex with amylopectin sufficient to cause precipitation. In general, ascorbyl palmitate resulted in the highest complexation, followed by retinyl palmitate and phytosterol ester. The presence of native lipids in high amylose maize starch did not inhibit complex formation. On the contrary, native lipids appear to increase the complexation yield and thermal stability of the starch–fatty acid ester inclusion complexes. The results of this study suggest that the formation of starch inclusion complexes with fatty acid esters seems to be limited by the solubility of the compound in the reaction medium and the structure of the molecule forming the ester with the fatty acid.

1. Introduction

The ability of some phytochemicals to provide health benefits makes these compounds attractive to consumers (Cohen, Orlova, Kovalev, Ungar & Shimoni, 2008), resulting in an increased interest in bioactive compounds in foods (Shimoni, 2009). For example, phytosterols, found in fruits and vegetables, are well known to reduce low density lipoprotein-cholesterol levels lowering the risk of cardiovascular diseases (Moreau & Hicks, 2004). However, many bioactive compounds, e.g. vitamins, are sensitive to thermal and oxidative stress and can be easily degraded during processing, storage, or in the gastrointestinal tract after consumption. Encapsulation can increase the stability of these compounds, may protect them from the acidic environment of the stomach, and insure their release in the small intestine where they are absorbed into the blood stream (Shimoni, 2009). This type of controlled release may also prevent the perception of undesirable sensory attributes (bitterness, astringency, etc.) associated with some bioactive compounds.

The use of starch in the pharmaceutical industry has grown in recent years (Eliasson & Wahlgren, 2004; Freire, Fertig, Podzeck, Veiga & Sousa, 2009; McConnell, Tutas, Mohamed, Banning & Basit, 2007; Milojevic et al., 1996a, 1996b; Podczeck & Freire, 2008). Properties such as biodegradability, low toxicity, food grade, availability (Öngen, Yilmaz, Jongboom & Feil, 2002), and physicochemical properties specific to starch, including retrogradation, film forming ability, complex formation, and resistance to various degrees towards amylase hydrolysis, make starch a promising material for delivery systems.

Amylose is well known to form inclusion complexes with some molecules such as iodine, alcohols, fatty acids, aromas (Rondeau-Mouro, Bail & Buléon, 2004), dimethyl sulfoxide (DMSO) (Godet, Tran, Colonna, Buleon & Pezolet, 1995), salicylic acid and its analogues (Oguchi, 1998; Uchino, Tozuka, Oguchi & Yamamoto, 2002), *p*-aminobenzoic acid (Tozuka et al., 2006), ibuprofen, and warfarin (Hong, Soini, Baker & Novotny, 1998). In the presence of these molecules, amylose forms a left-handed single helix stabilized by hydrogen bonds (Conde-Petit, Escher & Nuessli, 2006), with a hydrophilic outside surface and a hydrophobic inside helical channel (Immel & Lichtenthaler, 2000). Amylose single helices can arrange forming a crystalline structure known as V-type (Biais, Le Bail, Robert, Pontoire & Buléon, 2006). Guest molecules are usually included within the helix, but can also be trapped between helices (Rondeau-Mouro et al., 2004).

Even though the formation of amylose inclusion complexes with a wide variety of molecules has been known for many years, only recently, have these inclusion complexes been seriously investigated as a delivery system of non-drug bioactive compounds (Cohen et al., 2008; Lalush, Bar, Zakaria, Eichler & Shimoni, 2005; Lesmes, Barchechath & Shimoni, 2008; Lesmes, Cohen, Shener & Shimoni, 2009; Zabar, Lesmes, Katz, Shimoni & Bianco-Peled, 2009), including conjugated linoleic acid (Lalush et al., 2005; Yang, Gu

* Corresponding author. Tel.: +1 814 863 2960; fax: +1 814 863 6132.
E-mail address: grz1@psu.edu (G.R. Ziegler).

0144-8617/$ – see front matter © 2010 Elsevier Ltd. All rights reserved.
doi:10.1016/j.carbpol.2010.10.055

& Zhang, 2009) and genistein (Cohen et al., 2008). These investigations suggested that inclusion complexes can protect these compounds during their passage through the stomach, and be released in the small intestine by the action of enzymes on the amylose complexes (Lalush et al., 2005; Yang et al., 2009).

The formation of amylose–inclusion complexes depends on the size, shape, and solubility of guest molecules. If guest molecules are too water soluble, for example ascorbic acid, then they will not effectively partition into the starch matrix. In other cases, if molecules are too large, for example retinol or phytosterols, then they will not fit within the helical cavity that amylose forms when complexing with the ligands. Given the well known ability of amylose to form inclusion complexes with fatty acids, the use of fatty acid esters of these compounds may be an interesting approach for the formation of inclusion complexes with these bioactive molecules.

Encapsulation of bioactive compounds using a commercial native starch would be of relevance because of the lower cost as compared to prepared amylose (Tapanapunnitikul, Chaiseri, Peterson & Thompson, 2008). However, lipids present in native starch can interfere with starch complexation, for example with iodine (Hizukuri, Abe & Hanashiro, 2006). In other cases, the presence of native lipids can favor complex formation, such is the case with low solubility flavors (Tapanapunnitikul et al., 2008).

The objectives of the present study were to: (a) investigate the formation of amylose and high amylose starch inclusion complexes with the fatty acid esters ascorbyl palmitate (AP), retinyl palmitate (RP), and phytosterol esters (PE); and (b) evaluate the effect of native lipids and ligand concentration on the formation of high amylose starch–fatty acids ester inclusion complexes.

2. Materials and methods

2.1. Materials

High amylose maize starch (Hylon VII) was supplied by National Starch and Chemical Company (Bridgewater, NJ). AP, RP, DMSO, d_6-DMSO were obtained from Sigma–Aldrich, Inc (St. Louis, MO). PE were CoroWise™ plant sterol esters donated by Cargill Incorporated (Wayzata, MN), with the following composition: 30–60% sitosterol, 20–30% campesterol, 15–30% stigmasterol, <10% other sterols and 92.4% total sterols (Bohn et al., 2007).

2.2. Sample preparation

Defatted Hylon VII starch was produced by dispersing the starch in 90% DMSO aqueous solution followed by ethanol precipitation as described by Klucinec and Thompson (1998). Amylose and amylopectin fractions of Hylon VII were obtained by differential alcohol precipitation as described by Klucinec and Thompson (1998).

Starch inclusion complexes were prepared by the DMSO method as described by Godet, Buléon, Tran, and Colonna (1993) with slight modifications. A sample of 0.5 g of amylose, amylopectin, native or defatted Hylon VII was dispersed in 10 mL of a 95% DMSO aqueous solution in a boiling water bath with constant stirring for at least 1 h. Then, 1 mL of a fatty acid ester solution (1:10 weight guest molecule:weight starch) in 95% DMSO was mixed with the starch solution at 90 °C. The sample was kept at 90 °C in a water bath, and after 1 h, 25 mL of water at 90 °C was added to the sample and mixed. The water bath was turned off and samples were allowed to cool for 24 h (final temperature 28 °C). Inclusion complexes were recovered by centrifugation, washed three times with 40 mL of a 50/50 ethanol/water solution, then washed with 100% ethanol, filtered, rinsed with excess ethanol, and dried at room temperature in a desiccator. Dried samples were weighed and stored at −15 °C until used. Yields of the precipitates were calculated as grams of precipitate divided by the total amount of starch and fatty acid ester used, multiplied by 100.

Native Hylon VII starch inclusion complexes were also prepared using various amounts of fatty acid esters (2.5–50% (w/w) Hylon VII) to evaluate the effect of the amount of fatty acid ester added during processing on complex formation.

2.3. Wide angle X-ray diffraction

Wide angle X-ray diffraction patterns were obtained with a Rigaku MiniFlex II desktop X-ray diffractometer (Rigaku Americas Corporation, TX). Samples were equilibrated for 48 h over a saturated aqueous solution of KCl at room temperature (~85% relative humidity). Samples were exposed to a Cu Kα radiation and continuously scanned between 4° and 30° at a scan speed of 1°/min with a step size of 0.02° (λ = 0.15 nm). A current of 15 mA and 30 kV were used. Data was analyzed with Jade v.8 software (Material Data Inc., Livermore, CA).

To calculate the percentage of crystallinity (% crystallinity), an amorphous halo was subtracted from the overall X-ray diffraction pattern. The overall area was calculated as the area between the linear baseline and data points. The amorphous halo was generated by Jade software using the cubic spline fit option. The % crystallinity was calculated as the proportion of the crystalline area to the overall area multiplied by 100 (Creek, 2007; Evans, 2005; Rindlav, Hulleman & Gatenholm, 1997).

The relative crystal size of inclusion complexes was estimated from the broadening of the main peak reflections at 2θ around 13° and 20° by Jade software after peak decomposition, using the Scherrer's equation (Eq. (1)):

$$D_{(hkl)} = \frac{0.9 \times \lambda}{\beta_{1/2} \times \cos\theta} \quad (1)$$

where $D_{(hkl)}$ is the mean crystal size, λ represents the wave length of the X-ray used, $\beta_{1/2}$ is the full width at half maximum, and θ is the Bragg angle (Hizukuri & Nikuni, 1957). Peak reflections at $2\theta \approx 13°$ and $2\theta \approx 20°$ correspond to the planes (1 3 0) and (3 1 0) of the V_{6I} orthorhombic unit cell, respectively (Le Bail, Rondeau & Buléon, 2005; Rondeau-Mouro et al., 2004; Yamashita, 1965).

2.4. Thermal analysis

Approximately 5 mg of sample was weighed in a 60 μL stainless steel differential scanning calorimeter (DSC) pan (Perkin-Elmer Instruments, Norwalk, CT) and water was added to obtain a 10% dispersion (w/w). Pans were hermetically sealed and stored overnight for moisture equilibration. Samples were equilibrated to 10 °C, and then heated to 180 °C at 10 °C/min in a Thermal Advantage Q100 DSC (TA Instruments, New Castle, DE). The DSC was calibrated with indium, and an empty sample pan was used as a reference. The baseline was obtained by processing two empty pans using the same heating treatment and subtracted from the data. Data was analyzed using the TA Universal Analysis software (Universal Analysis 2000 v.4.2E, TA Instruments-Waters LLC, New Castle, DE).

2.5. Quantification of complexed fatty acid esters by Fourier transformed infrared (FTIR) spectroscopy

The amount of complexed fatty acid esters was estimated using a Bruker IFS 66/S FTIR Spectrometer (Bruker Optics, Billerica, MA). Approximately 3–5 mg of sample was rigorously mixed with a preweighed amount of KBr for 30 s using a Wig-L-Bug amalgamator, and 70 mg of this mixture was pressed into a pellet using a Quick Press (International Crystal Laboratories). Spectra were obtained in

transmission mode from 500 cm^{-1} to 4000 cm^{-1} at a resolution of 6 cm^{-1}.

Quantity of entrapped molecules in starch was calculated by subtracting the starch FTIR spectra from the inclusion complex spectra after water vapor correction. After subtraction, the area under the peak corresponding to the carbonyl group was calculated and normalized to 1 mg of sample. For RP and PE, the carbonyl peak was around 1738 cm^{-1} and 1737 cm^{-1}, respectively. For AP, two overlapping carbonyl peaks were identified between 1715 cm^{-1} and 1800 cm^{-1} and the combined area under the two peaks was used for quantification.

Preliminary experiments showed that ethanol washing was not sufficient to remove uncomplexed PE. Therefore, PE samples were washed with hexane before quantification. Approximately 10 mg of precipitate was washed with 100 μL hexane for 20 min, and then with 200 μL hexane. Samples were collected by centrifugation and stored in a desiccator until use.

Calibration standard curves were generated using physical mixtures of the fatty acid esters with native Hylon VII at concentrations from 0.5% to 10% (w fatty acid ester/w dry starch). To prepare standard mixtures, fatty acid esters were dispersed in ethanol, then Hylon VII was mixed into this dispersion, and finally, ethanol was evaporated.

2.6. Nuclear magnetic resonance (NMR)

AP–Hylon VII inclusion complexes were characterized using ^1H NMR as described by Wulff, Avgenaki, and Guzman (2005) with slight modifications. Approximately 25 mg of sample were dissolved in 0.7 mL of d_6-DMSO at 60 °C in a water bath for 40 min mixing every 8 min using a vortex. ^1H spectra were obtained at 400.13 MHz on a Bruker DRX-400 NMR spectrometer operating in the quadrature mode at 25 °C using 30° pulses and 8.95 s between scans to guarantee complete relaxation and quantitative integration. Spectra were referenced to the residual ^1H signal of d_6-DMSO (≏ = 2.49 ppm). The percentage of AP in the sample was calculated from the integration of the proton signal corresponding to the CH_3 from the end of the alkyl chain between 0.80 ppm and 0.88 ppm in relation to the integration of the proton signal of carbon 1 of the anhydroglucose units (AGU) between 4.95 ppm and 5.20 ppm.

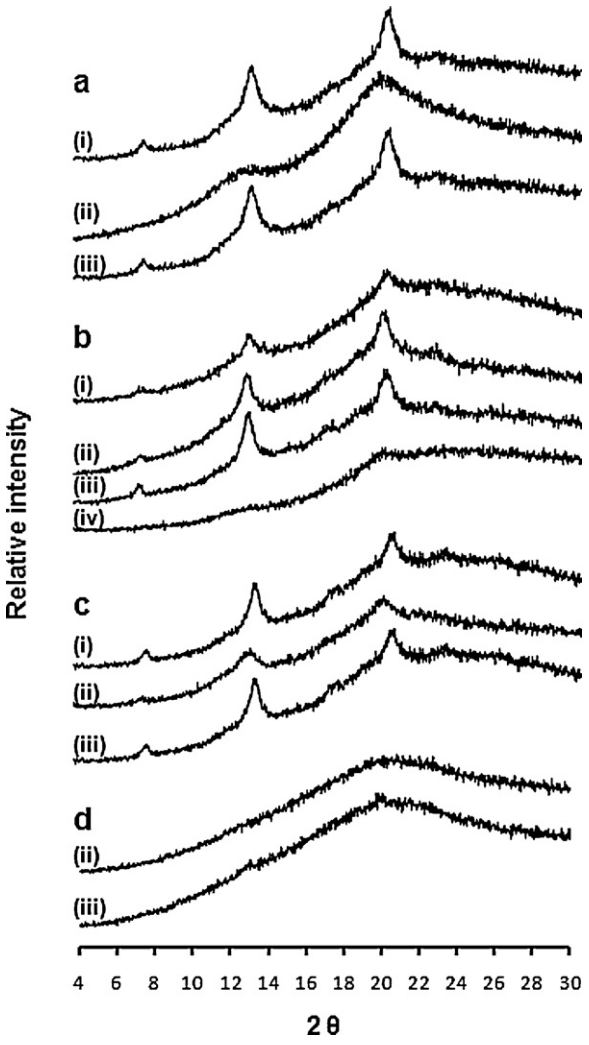

Fig. 1. X-ray diffraction patterns of (a) ascorbyl palmitate, (b) retinyl palmitate, (c) phytosterol ester, and (d) control (no fatty acid ester added) samples made with (i) amylose, (ii) defatted Hylon VII, (iii) native Hylon VII, and (iv) amylopectin.

3. Results and discussion

3.1. Inclusion complexes with amylose and amylopectin

AP, RP, PE all induced amylose precipitation. However, amylopectin precipitated only in the presence of RP. Even so, this cannot rule out the possibility of adsorption of some of the guest compounds to the amylopectin molecule or the complexation of guest compounds with external amylopectin chains. Based on the presence of V-type X-ray diffraction patterns, amylose formed inclusion complexes with all three fatty acid esters (Fig. 1a(i), b(i), and c(i)). A V-type diffraction pattern is usually associated with type II inclusion complexes (Biliaderis, 1992; Biliaderis & Galloway, 1989). However, Seneviratne and Biliaderis (1991) reported that freeze-dried and rehydrated type I inclusion complexes can display a diffused V-type pattern. In the present investigation, complexes were dried and then equilibrated at 85% relative humidity, so the possibility that these complexes are type I cannot be eliminated.

The highest yields of precipitate were observed for samples made with AP, followed by RP, and then by PE (Table 1). The alkyl chain of fatty acid esters is presumed to be included inside the heli-

Table 1
Yield, % crystallinity, % entrapped fatty acid ester, and stoichiometry of amylose and amylopectin precipitates with ascorbyl palmitate, retinyl palmitate, or phytosterol esters[x].

Fatty acid ester	Yield of precipitate (g precipitate/100 g starch + fatty acid ester)		% Crystallinity		% fatty acid ester in precipitate (w/w, dry starch)[y]		mol AGU/mol complexed fatty acid ester[z]	
	Amylose	Amylopectin	Amylose	Amylopectin	Amylose	Amylopectin	Amylose	Amylopectin
Ascorbyl palmitate	61.7 ± 0.3a	No precipitate	35 ± 3a	NA	6.3 ± 0.05a	NA	41	NA
Retinyl palmitate	11.2 ± 0.8b	2.3	23 ± 2b	15.8 ± 8.4	1.4 ± 0.35b	0.49 ± 0.10	228	991
Phytosterol ester	6.5 ± 0.4c	No precipitate	29 ± 1ab	NA	0.7 ± 0.01b	NA	576	NA

NA: not available because no precipitate was obtained; AGU: anhydroglucose units.
[x] Within column, mean ± standard deviation followed by different letter are significantly different at $\alpha = 0.05$.
[y] Reported values of % ascorbyl palmitate in precipitate are the adjusted FTIR values.
[z] Stoichiometry of phytosterol ester complexes was calculated based on sitosterol oleate molecular weight.

cal cavity similar to the currently accepted model for amylose–fatty acid inclusion complexes (Godet et al., 1995). Godet et al. (1995) reported a yield of 96.6% complexed amylose when 10% palmitic acid (w/w, amylose) was used. In the present investigation, only 61.7% yield was obtained when complexed with 10% AP (w/w, amylose). The weight fraction of palmitic acid in AP is around 0.62. Thus, the lower yield of amylose–AP precipitates is likely due to the lower proportion of added palmitic acid. The yield of amylose complexes with RP was 11.2% and with PE was 6.5%. The weigh fraction of fatty acids in RP and PE is 0.49 and 0.40, respectively. Therefore, the low yield of amylose complexes with these compounds was not only caused by the lower proportion of fatty acids.

Tapanapunnitikul et al. (2008) reported little yield of precipitate when low solubility compounds were used. These authors proposed that a lower solubility of molecules in the reaction medium results in less available molecules for complexation, and shorter and less stable complexes. Individual complexes with lower stability will be less likely to induce nucleation and further crystallization, resulting in lower precipitation. AP is an ester of palmitic acid with a hydrophilic ascorbic acid molecule (solubility: $\sim 3.3 \times 10^4$ mg ascorbic acid/100 mL water (Budavari, O'Neil, Smith, & Heckelman, 1989)). On the other hand, RP and PE are esters of fatty acids with hydrophobic molecules (solubility: ~1.7–1.8 mg retinol/100 mL water (Budavari et al., 1989) and 0.2 mg sterol/100 mL water (Szuts & Harosi, 1991)). Thus, the higher solubility of AP as compared to the other guest molecules could be one of the major reasons of the much higher yield of amylose–AP precipitates.

The % crystallinity was 35%, 23%, and 29% for amylose–AP, –RP, and –PE complexes, respectively (Table 1). The observed percentages of crystallinity were within the range previously reported for V-type starch (Evans, 2005). The % crystallinity depends on the ability of individual complexed amylose helices to pack into a crystallite. The difference in the ability of single helices to arrange into an ordered structure could be the result of the structure of the molecule forming the ester with the fatty acid. The small ascorbic acid molecule is less likely to significantly disturb the packing of single helices resulting in a higher % crystallinity. On the other hand, the larger and more flexible retinol molecule is more likely to interfere in the packing of helices.

Amylose–AP precipitates showed a single endotherm around 100 °C (Fig. 2a(i)) which can be attributed to the dissociation of inclusion complexes (Biliaderis & Seneviratne, 1990; Karkalas, Ma, Morrison & Pethrick, 1995; Raphaelides & Karkalas, 1988; Seneviratne & Biliaderis, 1991). Type II amylose–palmitic acid complexes have been reported to dissociate around 118 °C (Tufvesson, Wahlgren & Eliasson, 2003b). Thus, if amylose–AP complexes are type II, then these complexes had a lower thermal stability compared to its palmitic acid counterpart.

The polar head of the lipid can affect the thermal transition of amylose–lipid complexes (Eliasson, 1994). For example, amylose–monoglyceride complexes have a lower dissociation temperature as compared to their amylose–fatty acid counterparts (Tufvesson, Wahlgren, & Eliasson, 2003a; Tufvesson et al., 2003b). Similarly, the polar head of AP may have affected the thermal stability of helical complex between amylose and the aliphatic chain. It is possible that AP forms shorter helices with amylose, therefore lowering the dissolution temperature, as compared to palmitic acid complexes, due to higher steric interactions caused by the ascorbyl group.

Le Bail, Buleon, Shiftan & Marchessault (2000) proposed that in amylose–fatty acid complexes, the lipid could be in a *trans-gauche* conformation with the result that part of the lipid remains outside the helix. The presence of this conformation could depend on crystallization conditions and the necessity of locating the carboxylic head outside the helix. The ascorbyl head group of AP may favor the surrounding hydrophilic environment more so than the carboxylic group of palmitic acid. This may increase the probability of locating the head group outside of the hydrophobic helical cavity, favoring a *trans-gauche* conformation of the alkyl chain and resulting in a shorter amylose helix.

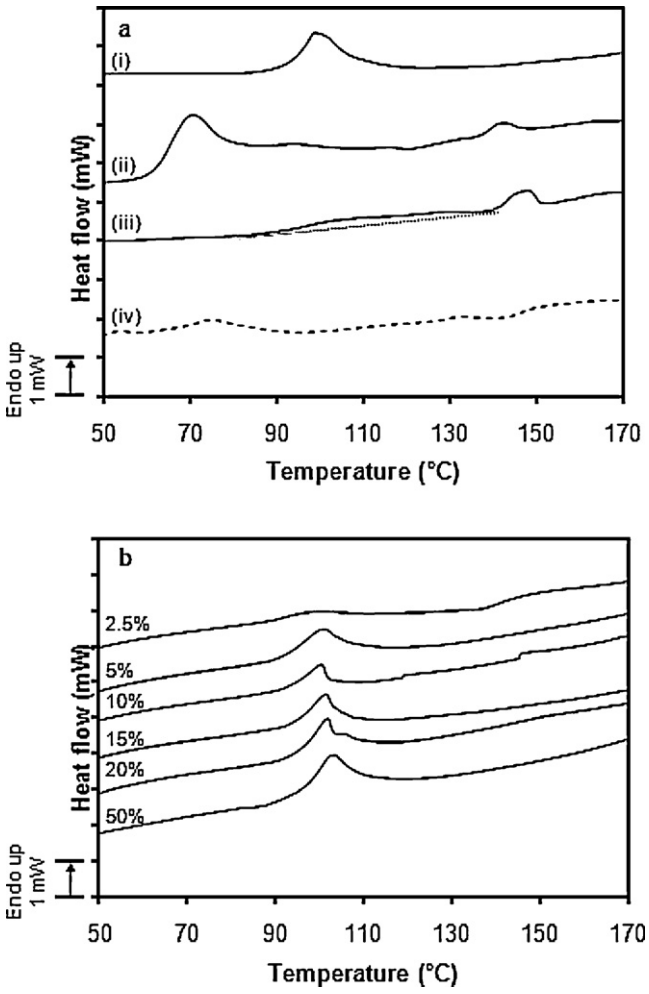

Fig. 2. DSC curves of: a(i) amylose–ascorbyl palmitate, a(ii) amylose–retinyl palmitate, a(iii) amylose–phytosterol ester; and a(iv) amylopectin–retinyl palmitate complexes. Part (b) shows DSC curves of inclusion complexes of native Hylon VII with various proportions of ascorbyl palmitate.

Although RP also has a C16 hydrocarbon chain to form inclusion complexes, amylose–RP complexes showed a much lower dissociation temperature (68.9 ± 2.8 °C) as compared to amylose–AP complexes (Fig. 2a(ii)). The low dissociation temperature may be the result of shorter helices formed due to a much stronger steric effect caused by the large retinol molecule forming the ester with palmitic acid. The necessity of placing the retinol molecule outside the helix may also promote the *trans-gauche* conformation of the alkyl chain a described by Lebail et al. (2000).

Thermograms of amylose–PE complexes showed a broad and flat endotherm between 85 °C and 135 °C (Fig. 2a(iii)). According to the manufacturer, PE were composed of approximately 40% by weight canola oil fatty acids, which are mainly unsaturated fatty acids: approximately 62% of oleic (C18:1), 21% of linoleic (C18:2), and 8% of linolenic acid (C18:3) (Warner, Orr, Parrott & Glynn, 1994). Therefore, it would be expected that the various fatty acids would produce different structures of inclusion complexes, such as helices with various lengths. The observed wide endotherm is in agreement with the dissociation temperatures of amylose inclusion complexes with C18:1, C18:2, and C18:3 fatty acids, which are

around 103–112 °C (Karkalas et al., 1995; Tufvesson et al., 2003b), 94–103 °C (Karkalas et al., 1995; Lalush et al., 2005; Tufvesson et al., 2003b), and 87–95 °C (Karkalas et al., 1995; Tufvesson et al., 2003b), respectively. Karkalas et al. (1995) observed that the dissociation endotherm of mixed acid complexes was broad with a peak melting temperature between the melting temperatures of the monoacid complexes. The composition of PE by mainly unsaturated fatty acids could have also contributed to the lower yield of the precipitate. Unsaturated fatty acids are less effective on forming inclusion complexes as compared to their saturated counterparts (Hahn & Hood, 1987; Karkalas & Raphaelides, 1986; Zabar et al., 2009).

Thermograms of RP and PE complexes (Fig. 2a(ii) and a(iii)) also showed an endotherm with peak temperature above 140 °C, which has been attributed to the dissociation of retrograded amylose (Raphaelides & Karkalas, 1988) or a structure formed by uncomplexed amylose chains (Biliaderis & Galloway, 1989; Biliaderis, Page, Slade & Sirett, 1985).

FTIR has been previously used to quantify the amount of complexed compounds that contain a carbonyl group (Biais et al., 2006; Fanta, Shogren & Salch, 1999; Uchino et al., 2002). For RP and PE samples, the carbonyl peak in the complexes and physical mixture (used to generate the calibration curve) resembled that of the pure compound. However the peaks corresponding to the carbonyl groups in AP complexes shifted slightly to a higher wave number (Fig. 3a). Thus, direct use of FTIR values may not provide an accurate determination of the amount of entrapped AP. The accuracy of the FTIR to estimate the amount of AP was evaluated with ^{1}H NMR. Based on the ^{1}H NMR results, the FTIR method underestimated the amount of entrapped AP giving values that were an average of 35% of the values estimated with the NMR. Hence, the percentages of AP entrapped in the complexes estimated by the FTIR were adjusted based on the NMR results.

A shift of the carbonyl peak of the FTIR spectra has been previously reported for amylose complexes with salicylic acid analogues (Uchino et al., 2002) and *p*-aminobenzoic acid (Tozuka et al., 2006). Uchino et al. (2002) attributed this shift to the breakage of hydrogen bonds between carboxyl groups of molecules of salicylic acid analogues in the crystalline state, so molecules can be included inside the amylose helix. A similar phenomenon possibly occurs when AP crystals are dissolved and molecules are included inside the helix. Alternatively, Tozuka et al. (2006) attributed the carbonyl band shift to the formation of hydrogen bonds between the carbonyl group of the guest and hydroxyl groups of amylose. It is possible that a similar interaction occurs between AP and amylose. However, steric constraints may prevent RP and PE from forming these hydrogen bonds, which could also contribute to the lower complexation efficiency of these two molecules.

The maximum % fatty acid ester in the precipitate (w fatty acid ester/w dry starch) was observed for AP (6.3%) followed by RP (1.42%) and by PE (0.73%) (Table 1). The proportion of the alkyl chain in the guest molecules could be responsible for some of the observed differences. The fatty acid weight fraction in AP, RP, and PE is 0.62, 0.49 and 0.40, respectively. However, differences in weight fractions are not large enough to solely account for the observed differences in the % fatty acid esters in the precipitates. The smaller size of AP molecules may allow the formation of more inclusion complexes within the same amylose chain, resulting in higher amount of AP entrapment per weight of amylose. Based on DSC curves, in addition to inclusion complexes, precipitates of RP and PE also contained uncomplexed amylose (peak around 140 °C in Fig. 2a(ii) and a(iii)). After precipitates were washed, this uncomplexed amylose most likely did not contain fatty acid esters, resulting in a lower % RP and PE in the precipitates (w/w, amylose). It is possible that PE precipitates had a larger ratio of uncomplexed:complexed amylose than that of RP samples, which resulted in a lower percentage of entrapment. This is in agreement with the larger ratio of uncomplexed:complexed amylose transition enthalpies (3.6 J/g:6.5 J/g) in PE precipitates compared to that of RP precipitates (1.7 J/g:14 J/g).

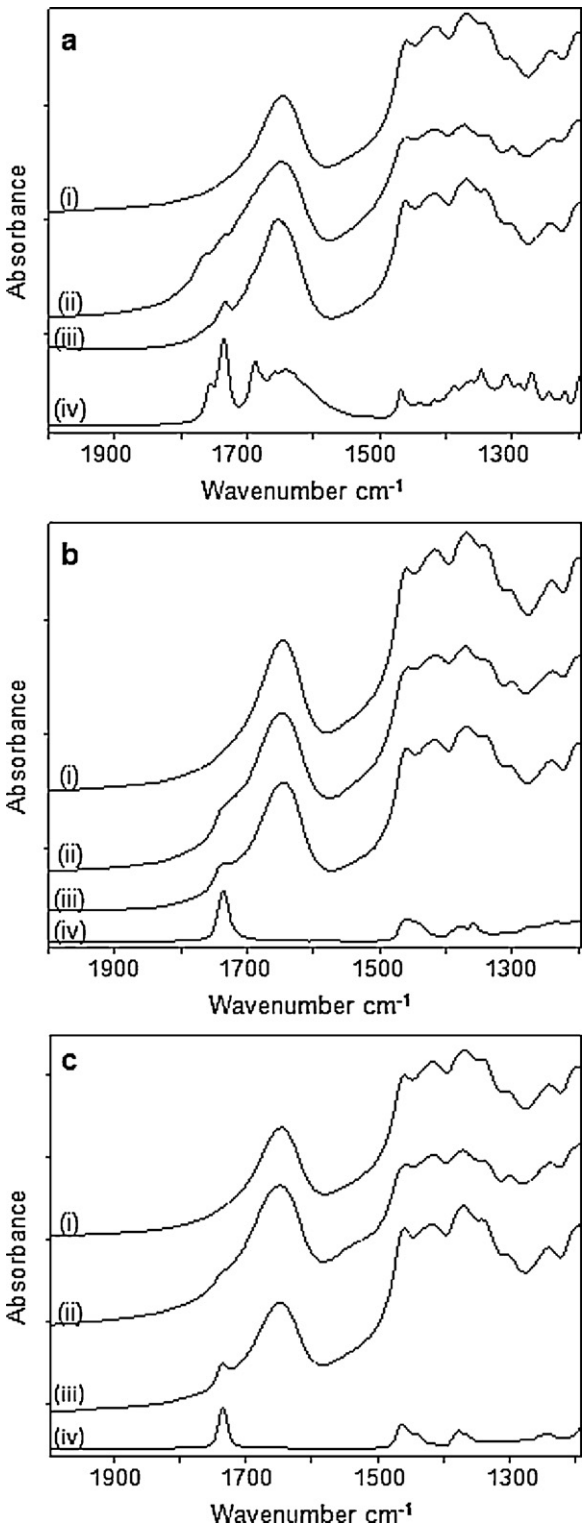

Fig. 3. FTIR spectra of (i) Hylon VII, (ii) Hylon II–fatty acid ester complex, (iii) Hylon VII–fatty acid ester physical mixture, and (iv) pure fatty acid esters in (a) ascorbyl palmitate, (b) retinyl palmitate, and (c) phytosterol ester samples.

Although AP showed a better complexing ability with amylose, AP did not induced amylopectin precipitation. Only RP produced an amylopectin precipitate, which showed a very weak V-pattern (Fig. 1b(iv)) indicating the formation of inclusion complexes. Evi-

dence that amylopectin may interact with lipids or surfactants has been previously reported (Eliasson & Ljunger, 1988; Evans, 1986; Gudmundsson & Eliasson, 1990; Hahn & Hood, 1987; Huang & White, 1993; Kim, Eliasson & Larsson, 1992; Nakazawa & Wang, 2004; Villwock, Eliasson, Silverio & BeMiller, 1999). It could be argued that these inclusion complexes were formed with a small fraction of amylose or intermediate material contaminating amylopectin samples. However, if this was the case, complexes with AP would have also been observed. The precipitate of RP with amylopectin had a similar dissolution temperature (76.2 ± 1.9 °C), and a lower % crystallinity and % RP (w/w, amylopectin) than its amylose counterpart.

3.2. Inclusion complexes with Hylon VII starch and the effect of native lipids

Precipitates were obtained with native and defatted Hylon VII with and without addition of fatty acid esters (Table 2). Based on the V-type X-ray diffraction patterns, all three fatty acid esters formed inclusion complexes with Hylon VII regardless of the presence of native lipid (Fig. 1).

Native high amylose maize starch contains approximately 1% monoacyl lipids (w/w, dry starch), mainly composed of palmitic, stearic, and linoleic acid, in the form of free fatty acids and lysophospholipids (Morrison, 1988). These lipids can form inclusion complexes with starch. Without fatty acid ester addition, the yield of precipitates was around 10% and 20% for defatted and native Hylon VII starch, respectively. Tapanapunnitikul et al. (2008) also reported a 10% yield difference between precipitates of native and lipid-free high amylose maize starch. These authors explained that starch can precipitate out of solution by simple retrogradation, and by complex formation between starch and native lipids or added guest molecules. In defatted Hylon VII samples without fatty acid ester addition, the obtained precipitates are likely retrograded starch. This was confirmed by the presence of a single endotherm above 150 °C observed in DSC curves (data not shown) associated with retrograded amylose (Raphaelides & Karkalas, 1988).

In native Hylon VII precipitates an endotherm around 103 °C, in addition to the retrograded amylose endotherm, was observed, which can be associated with type I amylose–lipid inclusion complexes (Karkalas et al., 1995; Tufvesson et al., 2003b). Endotherms around 70 °C and 125 °C could also be observed. The transition around 70 °C could be associated with amylopectin retrogradation. However, inclusion complexes between native lipids and amylopectin cannot be ruled out. Transition temperatures between 118 and 125 °C have been associated with type II amylose–lipid inclusion complexes (Tufvesson et al., 2003b), so the endotherm around 125 °C is likely associated with these structures.

The presence of native lipids did not significantly affect the yield, % crystallinity, or % fatty acid ester in RP samples, but increased their dissociation temperature (Table 2). Tapanapunnitikul et al. (2008) suggested that native lipids may form ternary complexes between starch, guest molecule, and native lipids. These authors explained that native lipids may induce complex formation with the starch more avidly than low solubility flavor compounds. They proposed that a stable amylose–lipid complex could induce the formation of a more extended complex with the flavor molecules. Similarly, it is possible that native lipids induced the formation of a longer helix with higher thermal stability in Hylon VII and RP.

Complexes formed with AP or PE also had significantly higher dissolution temperature when native lipids were present (Table 2). Similar to RP samples, it is possible that the formation of co-inclusion complexes of starch–fatty acid ester–native lipid resulted in longer helices with higher thermal stability.

The yield of AP and PE precipitates was significantly higher in the presence of native lipids (Table 2). The formation of isolated

Table 2
Yield, % crystallinity, % entrapped fatty acid ester, and dissociation temperature of native and defatted Hylon VII precipitates made with 10% retinyl palmitate, phytosterol ester, or ascorbyl palmitate (g/100 g starch)[x].

Fatty acid ester	Yield of precipitate (g precipitate/100 g starch + fatty acid ester)		% Crystallinity		% fatty acid ester in precipitate (w/w, starch)[y]		Dissociation peak temperature of inclusion complexes (°C)	
	Native Hylon VII	Defatted Hylon VII	Native Hylon VII	Defatted Hylon VII	Native Hylon VII	Defatted Hylon VII	Native Hylon VII	Defatted Hylon VII
Ascorbyl palmitate	57 ± 3a	50 ± 3b	30 ± 3a	27 ± 2a	4.3 ± 1.0a	3.4 ± 0.7a	100.4 ± 0.4a	98.2 ± 0.5b
Retinyl palmitate	24 ± 6a	20 ± 6a	26 ± 3a	21 ± 2a	0.8 ± 0.5a	2.5 ± 1.9a	102 ± 13.8a	80.2 ± 12.9b
Phytosterol ester	17 ± 3a	7 ± 2b	23 ± 7a	21 ± 1a	0.2 ± 0.1a	0.2 ± 0.1a	125.8 ± 0.8a	97.9 ± 4.6b
None (control)	20 ± 5a	10 ± 1b	10 ± 4	NA	NA	NA	103.8 ± 1.8	NA

NA: data not available.
[x] For the same analysis (yield, % crystallinity, or % fatty acid in precipitate), mean ± standard deviation ($n \geq 2$) followed by the same letter show no significant differences between native and defatted Hylon VII at $\alpha = 0.05$ as determined by analysis of variance.
[y] Reported values of % ascorbyl palmitate in precipitate are the adjusted FTIR values.

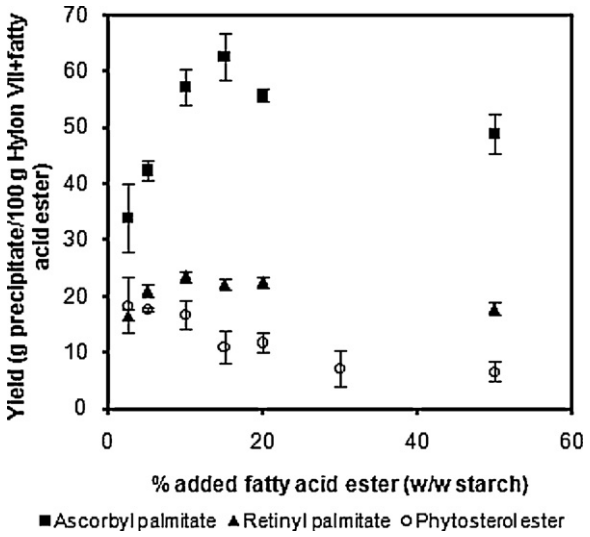

Fig. 4. Yield of native Hylon VII precipitates with various concentrations of ascorbyl palmitate, retinyl palmitate, or phytosterol esters. Error bars represent the standard deviation.

starch–native lipid inclusion complexes could be the reason of the higher yield. However, if that was the case, the % fatty acid ester in the precipitates would be lower due to a dilution effect. As suggested by Tapanapunnitikul et al. (2008) complex formation with certain compounds may be enhanced by the formation of ternary complexes with high amylose maize starch native lipids. Thus, native lipids may not only increase the thermal stability of the complexes, but also, the lipids may increase the partition of these fatty acid esters into the starch helix.

3.3. Effect of amount of added fatty acid ester

The yield of precipitate (g precipitate/100 g Hylon VII + fatty acid ester) depended on the fatty acid ester and concentration used (Fig. 4). Similar to amylose–guest complexes, the highest yield for Hylon VII–guest complexes was always observed for AP, followed by RP, and then by PE samples. The yield of AP or RP samples initially increased as higher amount of guest molecules were added, reaching a maximum at 15% w AP/w starch and 10% w RP/w starch. Above this concentration, addition of higher amounts of fatty acid esters resulted in lower yield. For PE precipitates, the maximum yield was observed at the lowest concentration used (2.5%) and appears to decrease above 10% added PE (Fig. 4).

The decrease in yield observed above a given amount of added compound could be due to a disruptive effect of high concentration of free fatty acid esters towards helical association. Lebail et al. (2000) proposed that at high free fatty acid content, lipids can get trapped in amylose chains without forming a complex. Similarly, the excess fatty acid esters can interact with polymer chains without forming a complex, which may reduce the availability of amylose segments and guest molecules to form inclusion complexes. Based on the size of these molecules, RP and PE are more likely to get trapped in polymer chains, and therefore, the disruptive effect toward complex formation possibly occurs at a lower concentration.

All precipitates had a V-type diffraction pattern similar to those shown in Fig. 1, indicating the formation of inclusion complexes. In AP samples, the % crystallinity increased as more AP was added in the reaction medium, while in RP precipitates, a maximum % crystallinity was reached at around 10–15% added RP. At 20% added RP, the % crystallinity decreased to about 20%, and higher addition of RP did not seem to significantly affect the % crystallinity. On the other hand, it appears that the % crystallinity of PE precipitates was not significantly affected by the amount of PE added during processing (Fig. 5).

The relative crystallite size estimated from the peak at $2\theta \approx 13^\circ$ appears to be larger when complexes were produced with lower proportion of fatty acid esters (Fig. 6a). The estimated size from the $2\theta \approx 13^\circ$ peak was generally larger than that from the $2\theta \approx 20^\circ$ peak (Fig. 6). Previous studies (Le Bail et al., 2005; Rondeau-Mouro et al., 2004; Yamashita, 1965) reported that the peak at $2\theta \approx 13^\circ$ corresponds to the (1 3 0) plane of the orthorhombic unit cell of V_6 crystals. For anhydrous *n*-butanol complexes, Yamashita (1965) observed no difference in the *d*-spacings of the (1 3 0) and (2 0 0) planes because of the pseudo-hexagonal nature of the unit cell of this complex, and therefore the reflection peak at $2\theta \approx 13^\circ$ corresponded to these two planes. The same author suggested that the growth rate in the (1 0 0) plane is faster than that in the (0 1 0) plane, and concluded that the longer side of the rectangular crystalline lamellae corresponds to the *a* axis of the unit cell. Similarly, it is possible that in the present study, the longer side of the crystals corresponded to the *a* axis of the unit cell, and the peak at $2\theta \approx 13^\circ$ corresponded to both the (1 3 0) and (2 0 0) planes, resulting in a larger crystal size than the size estimated from the $2\theta \approx 20^\circ$ peak.

The crystal size estimated from the $2\theta \approx 20^\circ$ reflection peak of RP and PE precipitates was not significantly affected ($p > 0.05$) by the % added fatty acid ester. On the other hand, the relative crystal size of AP precipitates increased with higher % added AP (Fig. 6b). At the highest AP concentration, the relative crystal size was roughly double the size of the crystals at low AP concentrations.

The amount of entrapped fatty acid ester varied depending on the type of fatty acid ester. The general trend for the three guest compounds was an increase in the entrapment of fatty acid esters in the precipitate as the amount of added guest molecules increased, with a tendency to reach a plateau at high concentrations of added fatty acid esters (Fig. 7). The higher entrapment at higher concentra-

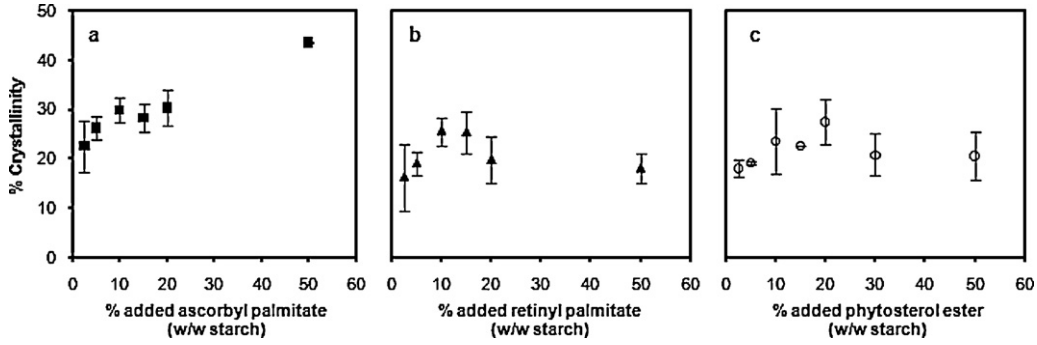

Fig. 5. Percentage of crystallinity of precipitates made from native Hylon VII and various concentrations of (a) ascorbyl palmitate, (b) retinyl palmitate, and (c) phytosterol esters. Error bars represent the standard deviation.

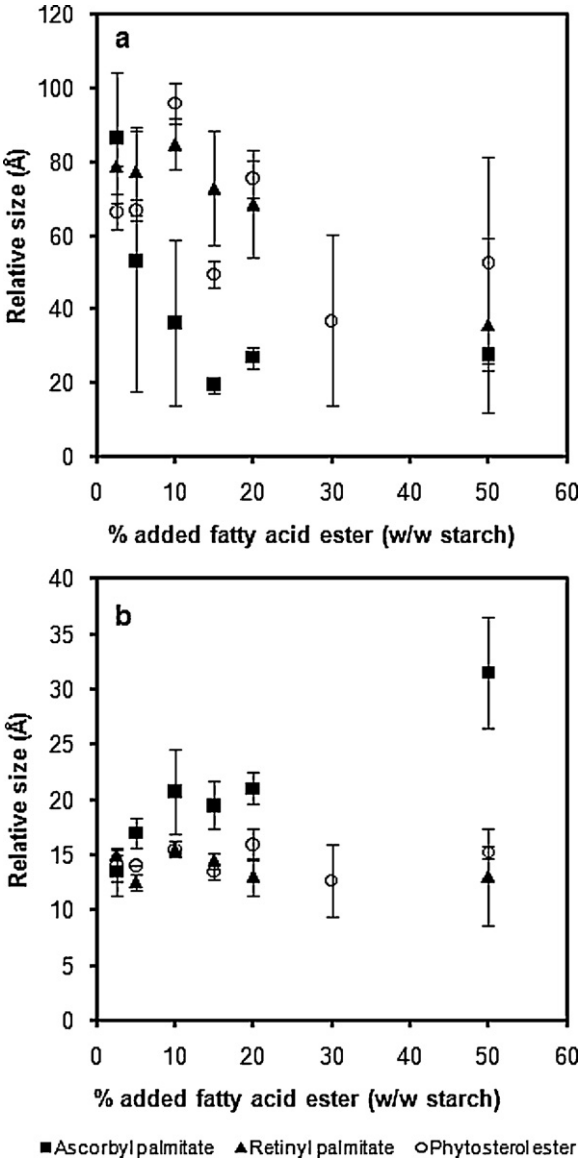

Fig. 6. Relative crystallite size estimated from the broadening of the main peak reflection at (a) $2\theta \approx 13^{\circ}$ and (b) $2\theta \approx 20^{\circ}$ of the X-ray diffraction pattern. Error bars represent the standard deviation.

tions of added fatty acid esters suggests that saturation of amylose chains were not a requisite for precipitation. This is contrary to the observations by Raphaelides and Karkalas (1988) where saturated amylose chains were preferentially removed from solution as compared to chains partially forming complexes with fatty acids.

The saturation molar ratio of amylose–palmitic acid complexes can be calculated based on the 2.014 nm length of the fatty acid alkyl chain (Karkalas & Raphaelides, 1986). Considering 6 AGU per helical turn with a pitch of 0.8 nm, the saturation molar ratio is 15.1 AGU per fatty acid molecule. Because AP is a monoester of palmitic acid, then its saturation molar ratio is also 15.1 AGU per AP molecule, which corresponds to 17% AP (w/w, AGU). At 50% added AP, the % AP in the precipitate was approximately 10% (Fig. 7a), therefore, at this maximum concentration, the % AP did not reach the calculated saturation concentration. As shown in Table 3, at this concentration, 24 AGU were needed to form a complex with one AP molecule. As proposed previously, amylose–AP complexes formed helices shorter than those of amylose–palmitic acid complexes. Thus, less than 15.1 AGU were forming the helix, and the remaining glucose residues were likely forming an amorphous region.

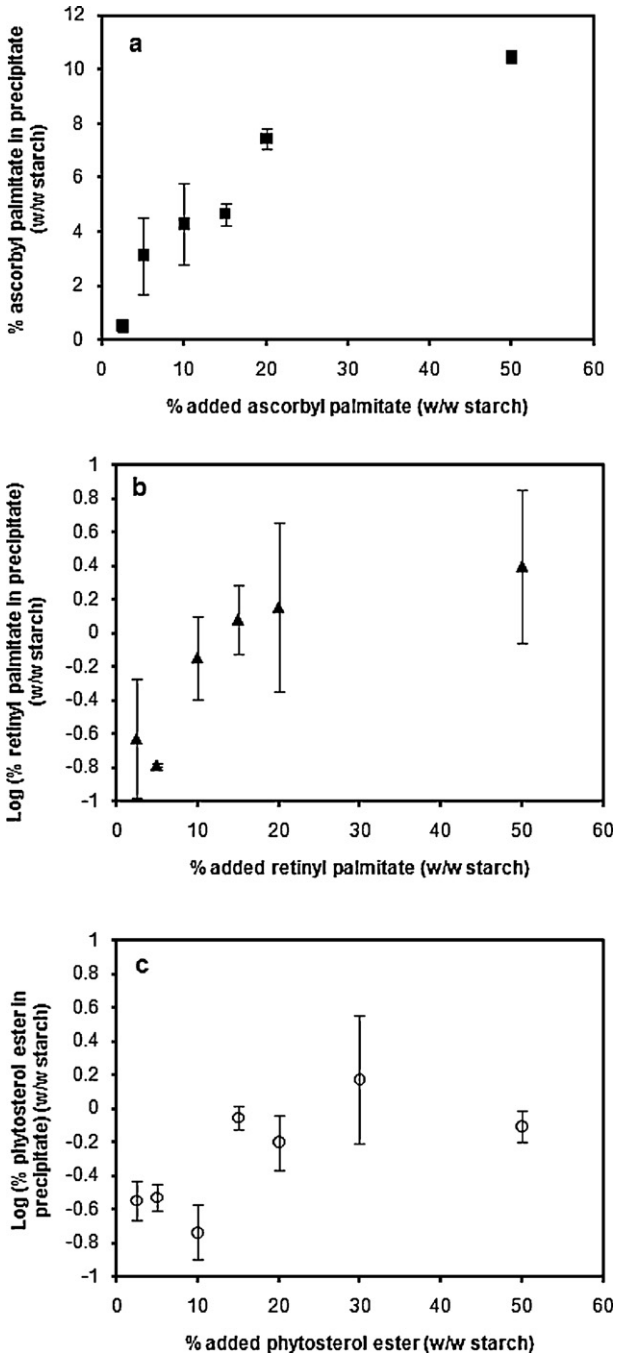

Fig. 7. Amount of fatty acid ester entrapped in precipitates of native Hylon VII with (a) ascorbyl palmitate, (b) retinyl palmitate, or (c) phytosterol ester. Error bars represent the standard deviation.

Table 3
Stoichiometry (mol AGU/mol fatty acid ester) of native Hylon VII–fatty acid ester inclusion complexes at various concentrations of added fatty acid ester.

% Added fatty acid ester	Ascorbyl palmitate	Retinyl palmitate	Phytosterol ester[a]
2.5	536	1600	1505
5.0	92	1971	1430
10	64	498	2396
15	55	295	478
20	34	348	698
50	24	65	541

[a] Calculated based on the molecular weight of sitosterol oleate.

High variability of the % entrapped RP and PE was observed. Based on regression analysis, a logarithmic transformation of the % of entrapped fatty acid ester was necessary to obtain a valid quadratic model for both RP ($R^2 = 0.81$) and PE ($R^2 = 0.85$). The amount of entrapped RP or PE seems to reach a plateau around 15–20% added fatty acid ester (Fig. 7b and c), likely due to the solubility limit of these molecules in the reaction medium.

A large proportion of the added fatty acid esters did not form inclusion complexes, even at low fatty acid ester:starch ratios. This is in agreement with previous studies in which free lipids were detected after palmitic acid (Le Bail et al., 2000; Raphaelides & Karkalas, 1988) and monoglycerides (Eliasson & Krog, 1985) were complexed with amylose in a DMSO solution, even when the ratio of amylose:lipid was increased. Competition between DMSO and lipid molecules to occupy the helical cavity (Raphaelides & Karkalas, 1988), and kinetic and steric factors (Le Bail et al., 2000) have been suggested as possible reasons why 100% complexation is not achieved.

Native Hylon VII–AP complexes disassociated between 85 °C and 130 °C, with a peak temperature around 99–103 °C (Fig. 2b). At lower AP concentrations, the peak disassociation temperature was around 100–101 °C. As the concentration of AP increased, a second peak around 102–103 °C appeared suggesting the presence of a second population of structures with slightly higher thermal stability. The higher dissociation temperature suggests the formation of a longer helical structure. In samples made with 50% AP, only a peak at around 102–103 °C could be observed.

Godet, Bouchet, Colonna, Gallant, and Buleon (1996) proposed that in amylose–palmitic acid complexes, two palmitic acid molecules arranged tail to tail are included in the helix. It is possible that at low concentration of AP, shorter helices with a lower dissociation temperature containing only one AP molecule were forming the crystals. As the concentration of AP increased, longer helices with higher thermal stability were formed possibly due to the inclusion of two AP molecules arranged tail to tail within the same helix, similar to the model proposed by Godet et al. (1996) for amylose–palmitic acid complexes.

Lower dissociation enthalpies were observed in samples made with lower % AP. Lower enthalpies are caused if part of the amylose remains uncomplexed (Raphaelides & Karkalas, 1988), which suggests that partially complexed amylose chains precipitated. These results are in agreement with the lower % crystallinity (Fig. 5a) and higher AGU/mol compound (Table 3) of samples made with lower % AP.

High variability in the thermal behavior of RP and PE inclusion complexes was observed between replicates and within samples (data not shown). Individual endotherms at various temperatures could be differentiated. In some measurements, these endotherms seemed to overlap forming a broad endotherm. These results suggest the formation of helical structures with various thermal stabilities.

In RP and PE samples, three endotherms were generally observed. In RP samples, a low temperature endotherm around 60–80 °C, medium temperature endotherm around 90–102 °C, and high temperature endotherm around 140–150 °C were identified. The high temperature endotherm 140–150 °C can be attributed to the dissociation of a structure formed by uncomplexed amylose (e.g. retrograded amylose) (Biliaderis et al., 1985). As described above, the endotherm around 60–80 °C is due to the dissolution of starch–RP complexes, while the endotherm around 90–102 °C may be associated with the dissolution of co-inclusion complexes of starch with RP and native lipids.

In PE samples, low temperature endotherms with a peak temperature around 60–70 °C, medium temperature endotherms between 94 and 126 °C, and the high temperature endotherm with a peak temperature above 138 °C were observed. Medium temperature endotherms (peak temperature between 104 and 126 °C) are in agreement with the melting transition observed for amylose–phytosterol complexes (Fig. 2a(iii)), while the endotherm above 138 °C is likely associated with structures formed by uncomplexed amylose. The low temperature transition was not caused by melting of uncomplexed PEs because DSC analysis of the pure compound showed that melting occurred below 60 °C. Thus, given the variety of fatty acids and sterols that formed the PE, it could be possible that some of the inclusion complexes are formed as shorter helices. It is also possible, that this low temperature endothermic transition represents the dissociation of type I inclusion complexes.

4. Conclusions

Selected fatty acid esters of bioactive compounds (ascorbic acid, retinol, and phytosterols) formed inclusion complexes with amylose. However, only RP formed complexes with amylopectin. Hylon VII starch could be used to form these inclusion complexes. In general, native lipids increased the yield of the precipitates and the thermal stability of the complexes, possibly caused by the formation of co-inclusion complexes of starch–fatty acid ester–native lipid. Formation of starch inclusion complexes with fatty acid esters seemed to be limited by the solubility of the compound in the reaction medium and the structure of the molecule forming the ester with the fatty acid.

Thus, Hylon VII–fatty acid ester inclusion complexes may have potential for the delivery of bioactive compounds. However, the formation of these complexes may be limited by the solubility and molecular structure of the specific compound forming the ester with the fatty acid.

Acknowledgements

This work was funded through The Pennsylvania Agricultural Experiment Station administered by The College of Agricultural Sciences of The Pennsylvania State University. The assistance of Dr. Alan Benesi with the NMR, and the assistance of Dr. Josh Stapleton from the Material Research Institute at the Pennsylvania State University with the FTIR are also gratefully acknowledged.

References

Biais, B., Le Bail, P., Robert, P., Pontoire, B., & Buléon, A. (2006). Structural and stoichiometric studies of complexes between aroma compounds and amylose. Polymorphic transitions and quantification in amorphous and crystalline areas. *Carbohydrate Polymers*, *66*(3), 306–315.

Biliaderis, C. G. (1992). Structures and phase-transitions of starch in food systems. *Food Technology*, *46*(6), 98–109, 145.

Biliaderis, C. G., & Galloway, G. (1989). Crystallization behavior of amylose–V complexes – structure property relationships. *Carbohydrate Research*, *189*, 31–48.

Biliaderis, C. G., Page, C. M., Slade, L., & Sirett, R. R. (1985). Thermal behavior of amylose–lipid complexes. *Carbohydrate Polymers*, *5*(5), 367–389.

Biliaderis, C. G., & Seneviratne, H. D. (1990). On the supermolecular structure and metastability of glycerol monostearate–amylose complex. *Carbohydrate Polymers*, *13*(2), 185–206.

Bohn, T., Tian, Q., Chitchumroonchokchai, C., Failla, M. L., Schwartz, S. J., Cotter, R., et al. (2007). Supplementation of test meals with fat-free phytosterol products can reduce cholesterol micellarization during simulated digestion and cholesterol accumulation by Caco-2 cells. *Journal of Agricultural and Food Chemistry*, *55*, 267–272.

Budavari, S., O'Neil, M. J., Smith, A., & Heckelman, P. E. (Eds.). (1989). *The Merck Index. An Encyclopedia of chemicals, drugs and biologicals*. Rahway, NJ, USA: Merck & Co., Inc.

Cohen, R., Orlova, Y., Kovalev, M., Ungar, Y., & Shimoni, E. (2008). Structural and functional properties of amylose complexes with genistein. *Journal of Agricultural and Food Chemistry*, *56*(11), 4212–4218.

Conde-Petit, B., Escher, F., & Nuessli, J. (2006). Structural features of starch–flavor complexation in food model systems. *Trends in Food Science & Technology*, *17*(5), 227–235.

Creek, J. A. (2007). Nanoscale self-assembly of starch: Phase relations, formation, and structure. In *Materials science and engineering*. University Park: The Pennsylvania State University., p. 235.

Eliasson, A. C. (1994). Interactions between starch and lipids studied by DSC. *Thermochimica Acta*, *246*(2), 343–356.
Eliasson, A. C., & Krog, N. (1985). Physical properties of amylose–monoglyceride complexes. *Journal of Cereal Science*, *3*, 239–248.
Eliasson, A. C., & Ljunger, G. (1988). Interactions between amylopectin and lipid additives during retrogradation in a model system. *Journal of the Science of Food and Agriculture*, *44*(4), 353–361.
Eliasson, A. C., & Wahlgren, M. (2004). Starch–lipid interactions and their relevance in food products. In A.-C. Eliasson (Ed.), *Starch in food* (pp. 441–460). Boca Raton, FL: CRC Press LLC.
Evans, A. (2005). Enzyme susceptibility of high-amylose starch precipitated from sodium hydroxide dispersions at different precipitation conditions. In *Food science*. University Park: The Pennsylvania State University., p. 196.
Evans, I. D. (1986). An investigation of starch/surfactant interactions using viscosimetry and differential scanning calorimetry. *Starch/Stärke*, *38*(7), 227–235.
Fanta, G. F., Shogren, R. L., & Salch, J. H. (1999). Steam jet cooking of high-amylose starch–fatty acid mixtures. An investigation of complex formation. *Carbohydrate Polymers*, *38*(1), 1–6.
Freire, A. C., Fertig, C. C., Podzeck, F., Veiga, F., & Sousa, J. (2009). Starch-based coatings for colon-specific delivery. Part I: The influence of heat treatment on the physico-chemical properties of high amylose maize starches. *European Journal of Pharmaceutics and Biopharmaceutics*, *72*, 574–586.
Godet, M. C., Bouchet, B., Colonna, P., Gallant, D. J., & Buleon, A. (1996). Crystalline amylose–fatty acid complexes: Morphology and crystal thickness. *Journal of Food Science*, *61*(6), 1196.
Godet, M. C., Buléon, A., Tran, V., & Colonna, P. (1993). Structural features of fatty acid–amylose complexes. *Carbohydrate Polymers*, *21*(2–3), 91–95.
Godet, M. C., Tran, V., Colonna, P., Buleon, A., & Pezolet, M. (1995). Inclusion/exclusion of fatty acids in amylose complexes as a function of the fatty acid chain length. *International Journal of Biological Macromolecules*, *17*(6), 405–408.
Gudmundsson, M., & Eliasson, A. C. (1990). Retrogradation of amylopectin and the effects of amylose and added surfactants/emulsifiers. *Carbohydrate Polymers*, *13*(3), 295–315.
Hahn, D. E., & Hood, L. F. (1987). Factors influencing corn starch–lipid complexing. *Cereal Chemistry*, *64*(2), 81–85.
Hizukuri, S., Abe, J., & Hanashiro, I. (2006). Starch: Analytical aspects. In A.-C. Eliasson (Ed.), *Carbohydrates in food* (pp. 305–390). Boca Raton, FL: CRC Taylor & Francis Group.
Hizukuri, S., & Nikuni, Z. (1957). Micelle dimensions of potato starch. *Nature*, *180*(4583), 436–437.
Hong, M., Soini, H., Baker, A., & Novotny, M. V. (1998). Complexation between amylodextrins olygomers and selected pharmaceuticals measured through capillary electrophoresis. *Analytical Chemistry*, *70*, 3590–3597.
Huang, J. J., & White, P. J. (1993). Waxy corn starch: Monoglyceride interaction in a model system. *Cereal Chemistry*, *70*(1), 42–47.
Immel, S., & Lichtenthaler, F. W. (2000). The hydrophobic topographies of amylose and its blue iodine complex. *Starch/Stärke*, *52*(1), 1–8.
Karkalas, J., Ma, S., Morrison, W. R., & Pethrick, R. A. (1995). Some factors determining the thermal properties of amylose inclusion complexes with fatty acids. *Carbohydrate Research*, *268*(2), 233–247.
Karkalas, J., & Raphaelides, S. (1986). Quantitative aspects of amylose–lipid interactions. *Carbohydrate Research*, *157*, 215–234.
Kim, H. R., Eliasson, A.-C., & Larsson, K. (1992). Dynamic rheological studies on an interaction between lipid and various native and hydroxypropyl potato starches. *Carbohydrate Polymers*, *19*(3), 211–218.
Klucinec, J. D., & Thompson, D. B. (1998). Fractionation of high-amylose maize starches by differential alcohol precipitation and chromatography of the fractions. *Cereal Chemistry*, *75*(6), 887–896.
Lalush, I., Bar, H., Zakaria, I., Eichler, S., & Shimoni, E. (2005). Utilization of amylose–lipid complexes as molecular nanocapsules for conjugated linoleic acid. *Biomacromolecules*, *6*(1), 121–130.
Le Bail, P., Buleon, A., Shiftan, D., & Marchessault, R. H. (2000). Mobility of lipid in complexes of amylose–fatty acids by deuterium and 13C solid state NMR. *Carbohydrate Polymers*, *43*(4), 317–326.
Le Bail, P., Rondeau, C., & Buléon, A. (2005). Structural investigation of amylose complexes with small ligands: Helical conformation, crystalline structure and thermostability. *International Journal of Biological Macromolecules*, *35*(1–2), 1–7.
Lesmes, U., Barchechath, J., & Shimoni, E. (2008). Continuous dual feed homogenization for the production of starch inclusion complexes for controlled release of nutrients. *Innovative Food Science & Emerging Technologies*, *9*(4), 507–515.
Lesmes, U., Cohen, S. H., Shener, Y., & Shimoni, E. (2009). Effects of long chain fatty acid unsaturation on the structure and controlled release properties of amylose complexes. *Food Hydrocolloids*, *23*(3), 667–675.
McConnell, E. L., Tutas, J., Mohamed, M. A. M., Banning, D., & Basit, A. W. (2007). Colonic drug delivery using amylose films: The role of aqueous ethylcellulose dispersions in controlling drug release. *Cellulose*, *14*, 25–34.
Milojevic, S., Newton, J. M., Cummings, J. H., Gibson, G. R., Louise Botham, R., Ring, S. G., et al. (1996a). Amylose as a coating for drug delivery to the colon: Preparation and in vitro evaluation using 5-aminosalicylic acid pellets. *Journal of Controlled Release*, *38*(1), 75–84.
Milojevic, S., Newton, J. M., Cummings, J. H., Gibson, G. R., Louise Botham, R., Ring, S. G., et al. (1996b). Amylose as a coating for drug delivery to the colon: Preparation and in vitro evaluation using glucose pellets. *Journal of Controlled Release*, *38*(1), 85–94.
Moreau, R. A., & Hicks, K. B. (2004). The *in vitro* hydrolysis of phytosterol conjugates in food matrices by mammalian digestive enzymes. *Lipids*, *39*(8), 769–776.
Morrison, W. R. (1988). Lipids in cereal starches: A review. *Journal of Cereal Science*, *8*(1), 1–15.
Nakazawa, Y., & Wang, Y.-J. (2004). Effect of annealing on starch–palmitic acid interaction. *Carbohydrate Polymers*, *57*, 327–335.
Oguchi, T. (1998). Structural change and complexation of strictly linear amylose induced by sealed-heating with salicylic acid. *Journal of the Chemical Society. Faraday Transactions*, *94*(7), 923.
Öngen, G., Yilmaz, G., Jongboom, R. O. J., & Feil, H. (2002). Encapsulation of α-amylase in a starch matrix. *Carbohydrate Polymers*, *50*(1), 1–5.
Podczeck, G. F., & Freire, A. C. (2008). *Coating Composition Comprising Starch*. WO/2008/012573, January 31.
Raphaelides, S., & Karkalas, J. (1988). Thermal-dissociation of amylose fatty–acid complexes. *Carbohydrate Research*, *172*(1), 65–82.
Rindlav, A., Hulleman, S. H. D., & Gatenholm, P. (1997). Formation of starch films with varying crystallinity. *Carbohydrate Polymers*, *34*, 25–30.
Rondeau-Mouro, C., Bail, P. L., & Buléon, A. (2004). Structural investigation of amylose complexes with small ligands: Inter- or intra-helical associations? *International Journal of Biological Macromolecules*, *34*(5), 251–257.
Seneviratne, H. D., & Biliaderis, C. G. (1991). Action of α-amylases on amylose–lipid complex superstructures. *Journal of Cereal Science*, *13*(2), 129–143.
Shimoni, E. (2009). Nanotechnology for foods: Delivery systems. In G. Barbosa-Canovas, A. Mortimer, D. Lineback, W. Spiess, K. Buckle, & P. Colonna (Eds.), *Global Issues in food science and technology* (pp. 411–424). United States: Elsevier Inc.
Szuts, E. Z., & Harosi, F. I. (1991). Solubility of retinoids in water. *Archives of Biochemistry and Biophysics*, *287*(2), 297–304.
Tapanapunnitikul, O., Chaiseri, S., Peterson, D. G., & Thompson, D. B. (2008). Water solubility of flavor compounds influences formation of flavor inclusion complexes from dispersed high-amylose maize starch. *Journal of Agricultural and Food Chemistry*, *56*(1), 220–226.
Tozuka, Y., Takeshita, A., Nagae, A., Wongmekiat, A., Moribe, K., Oguchi, T., et al. (2006). Specific inclusion mode of guest compounds analyzed by solid state NMR spectroscopy. *Chemical & Pharmaceutical Bulletin*, *54*(8), 1097–1101.
Tufvesson, F., Wahlgren, M., & Eliasson, A.-C. (2003a). Formation of amylose–lipid complexes and effects of temperature treatment. Part 1. Monoglycerides. *Starch/Stärke*, *55*, 61–71.
Tufvesson, F., Wahlgren, M., & Eliasson, A.-C. (2003b). Formation of amylose–lipid complexes and effects of temperature treatment. Part 2. Fatty acids. *Starch/Stärke*, *55*, 138–149.
Uchino, T., Tozuka, Y., Oguchi, T., & Yamamoto, K. (2002). Inclusion compound formation of amylose by sealed-heating with salicylic acid analogues. *Journal of Inclusion Phenomena and Molecular Recognition in Chemistry*, *43*(1), 31.
Villwock, V. K., Eliasson, A. C., Silverio, J., & BeMiller, J. N. (1999). Starch–lipid interactions in common, waxy, *ae du*, and *ae su2* maize starches examined by differential scanning calorimetry. *Cereal Chemistry*, *76*(2), 292–298.
Warner, K., Orr, P., Parrott, L., & Glynn, M. (1994). Effects of frying oil composition on potato chip stability. *Journal of the American Oil Chemists' Society*, *41*(10), 1117–1121.
Wulff, G., Avgenaki, G., & Guzman, M. S. P. (2005). Molecular encapsulation of flavours as helical inclusion complexes of amylose. *Journal of Cereal Science*, *41*, 239–249.
Yamashita, Y. (1965). Single crystals of amylose V complexes. *Journal of Polymer Science: Part A*, *3*, 3251–3260.
Yang, Y., Gu, Z., & Zhang, G. (2009). Delivery of bioactive conjugated linoleic acid with self-assembled amylose–CLA complex. *Journal of Agricultural and Food Chemistry*, *57*(15), 7125–7130.
Zabar, S., Lesmes, U., Katz, I., Shimoni, E., & Bianco-Peled, H. (2009). Studying different dimensions of amylose-long chain fatty acid complexes: Molecular, nano and micro level characteristics. *Food Hydrocolloids*, *23*(7), 1918–1925.